

CHARACTERIZING THE MICROSTRUCTURE OF DETERIORATED CEMENTITIOUS MATERIALS WITH X-RAY MICROTOMOGRAPHY

Michael Angelo Promentilla

Chemical Engineering Department, De La Salle University,
Manila, Philippines, Tel: +63(02)5360247, e-mail: michael.promentilla@dlsu.edu.ph

Received Date: November 27, 2010

Abstract

Cementitious material such as concrete is not only the most widely used infrastructure material, but it is also now being considered as an engineered barrier material for nuclear waste repository due to its structural strength and high confinement capacity for a long period of time. It is therefore imperative to understand how microstructure changes during deterioration to assess its long-term durability performance. This paper presents some applications of X-ray microtomography to examine the microstructure of deteriorated cementitious materials. X-ray microtomography is becoming an attractive option for nondestructive and noninvasive three-dimensional (3D) imaging of internal structure of materials. As this technique operates on the same basic principle of medical CT (computed tomography) scanners, it provides the 3D reconstruction of images from finite radiological images; but with much higher spatial resolution. For example, a microfocus X-ray CT system was used in our study to visualize the connected crack network of frost-induced damaged mortar at spatial resolution of orders of 10 μm . Moreover, synchrotron-based microtomography was also used to visualize at submicron level the pore spaces of mortar being deteriorated due to calcium leaching. Not only the CT images provide the qualitative information, but also these images allow us to make quantitative measurement of 3D parameters such as the connectivity and tortuosity. Representative samples from the analyzed 3D images were presented to demonstrate the said technique. Thus, these studies would serve as an impetus to further utilize X-ray microtomography in understanding the relationship between the microstructure and durability performance of these cementitious materials.

Keywords: Cementitious material, Microstructure, X-ray microtomography

Introduction

Cementitious materials such as mortar and concrete are widely used as construction materials in many infrastructures throughout the world. But despite its widespread use, fundamental understanding to its microstructure and long-term durability is still limited. Durability performance of concrete infrastructures must be assessed as it can be exposed to aggressive environment during the lifetime of the structure. For infrastructures commonly used in marine structures or as protective barrier in the underground disposal of long-lived nuclear waste, diffusion through the cracks or pores is the predominant transport mechanism that could influence its durability. For example, diffusion of calcium ions from a hydrated cement system is considered as a primary mechanism in the long-term degradation of concrete structures for nuclear waste repository whereas the ingress of chloride ion has been well recognized as the primary reason for the corrosion of rebar in reinforced concrete. Hence, investigation of the microstructure plays an important role in understanding the transport properties of these materials.

Optical and electron microscopy have been commonly used, for instance, as research tools to examine the microstructure of concrete. However, the destructive or invasive way of specimen preparation prior to imaging of the cross-section may produce problematic artifacts. In addition, the limitations of observing a two-dimensional (2D) section of a

three-dimensional structure from 2D microscopy must also be borne in mind. Thus, this study explored the application of X-ray microtomography, a powerful noninvasive and nondestructive three dimensional (3D) imaging technique, to investigate the microstructure of deteriorated cementitious material. It operates on the same principle of the medical computed tomography (CT) scanner but with much higher spatial resolution of the CT images. This technique has received considerable attention in materials research including cement and concrete (e.g., see [1-3] and references therein). In this paper, we report some of our findings from the analysis of CT images obtained from two different computed tomography (CT) system: the microfocus X-ray CT and the synchrotron-based microtomography.

Background of Methodology

Image Acquisition with X-ray CT

Acquisition of 3D images of internal structures can be done with the aid of computed tomography. Computed tomography (CT) is a technique for obtaining volumetric measurements of the X-ray attenuation coefficient, creating images that map the variation of the X-ray attenuation coefficient within objects. An X-ray beam is sent to the specimen and the transmitted beam is recorded on a detector. According to Beer-Lambert's law, the ratio of the number of transmitted to incident X-ray photons is related to the integral of the linear attenuation coefficient (LAC) of the material along the path that the photons follow through the specimen. The resulting image (or radiographs) is a superimposed information or projection of a volume in a 2D plane. To get the 3D information, radiographic projections of the specimen are taken at many angles or projection views. In medical CT scanners, this is commonly done by turning the X-ray source and the detector around the object (which in this case is a human patient). While in industrial CT scanners, which is particularly applied to inanimate objects, the specimen is the one being rotated while the X-ray source and detector are fixed in position. Once these projections are available, a reconstruction algorithm can be used to produce the contiguous two dimensional images which provide a discrete approximation of the distribution of X-ray attenuation coefficient within the volume of the imaged specimen. This two dimensional image is commonly referred to as slice because it corresponds to the cross-section of what would be seen if the specimen were sliced along the scan plane. Each slice is a matrix of voxels (volume element or 3D pixel) in which each voxel is associated with a gray scale value (GSV) that is related to the measured linear attenuation coefficient. For example, in an 8-bit CT image with voxels' GSV that ranges from 0 to 255, the higher the X-ray attenuation coefficient of the material component, the higher the GSV of the corresponding voxel is expected.

Since the linear attenuation coefficient (LAC) is a sensitive measure of atomic composition and density, CT technique could therefore provide nondestructive 3D visualization and characterization of internal structure without the time-consuming and difficult sectioning of specimen as being done in 2D X-ray microscopy techniques. As long as the spatial resolution could be made small with respect to the microstructural feature of interest, the volumetric image obtained from these measurements could provide valuable 3D structural information. Generally, to achieve the high resolution requirement for X-ray microtomography, there are two X-ray sources that can be used. The first one uses the polychromatic divergent beam produced by a microfocus X-ray tube and the second one uses the monochromatic parallel beam from synchrotron radiation (see Figure1).

The microfocus X-ray CT system we used is the TOSCANER-3000 μ hd. It primarily consists of a microfocus X-ray source, a specimen manipulator, an image intensifier (II)

detector coupled to a CCD camera, and an image processing unit. The X-ray source has a 5 μm focal point with an X-ray tube voltage that ranges from 20-225 kV. The source-to-specimen distance and source-to-detector distance can be varied to obtain the desired geometric magnification. The micromanipulator precisely positions the specimen table in the X-ray beams and rotates it under computer control through 360 degrees for projection data acquisition. The table position and motions and camera options are under the control of the host computer. The host computer receives the projection images and performs the data processing, and the image reconstruction using a built-in reconstruction program for cone beam geometry.

On the other hand, the synchrotron-based microtomography we used is the X-ray CT system at Spring-8. SPring-8 (Super Photon ring-8 GeV) is one of the largest third generation synchrotron radiation facility located at Hyogo, Japan and it has beam-lines (e.g., BL20XU/BL47XU) that support a very high resolution X-ray CT system. The system consists of an X-ray light source from the beam-line, double crystal monochromator, high precision rotation stage, and high resolution X-ray image detector [4]. For example, the available X-ray energy from BL20XU can be tuned within the range of 8-38 keV. For the purpose of our study, the X-ray energy was tuned to beam energy of 15-20 keV. Using a high precision rotation stage, the image was taken at different views through 180 degrees rotation. The transmitted images are then detected by X-ray imaged detector which consists of thin scintillator, optic system and CCD camera. Tomographic reconstruction is done using a public domain computer program in use at SPring-8, which employs the convolution back projection algorithm to generate the slice images.

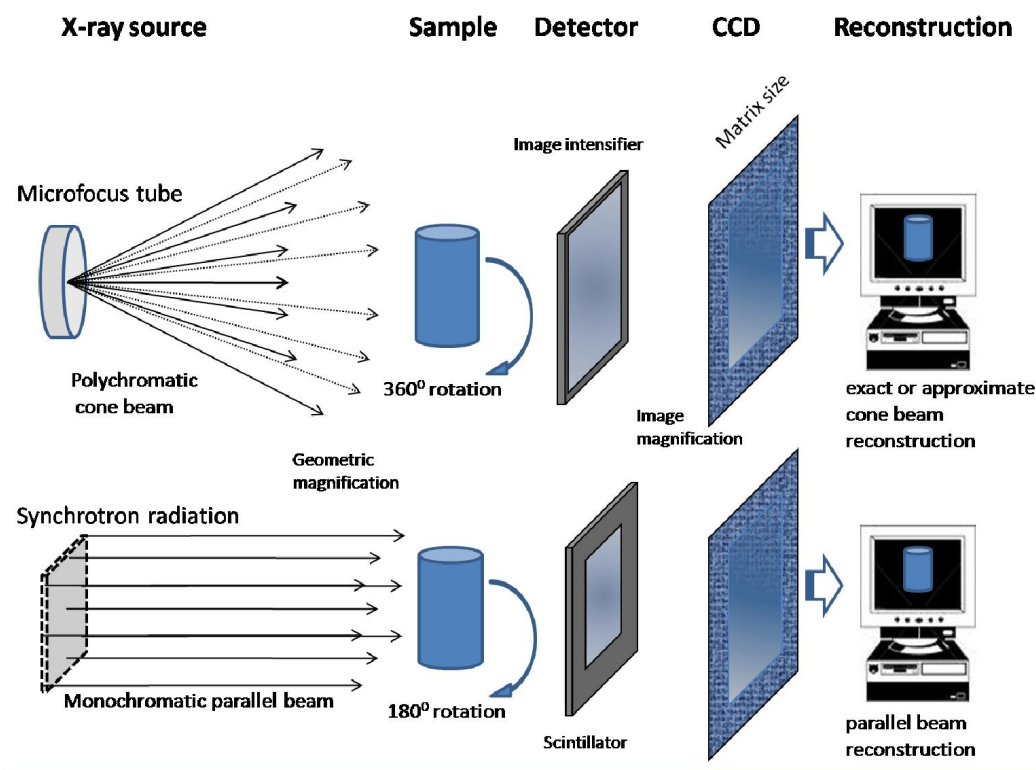


Figure 1. The schematic diagram of X-ray microtomography

3D Image Analysis

A number of image processing techniques and image analysis can be employed to CT images. These may include normalization or contrast stretching, noise suppression, and

smoothing, among others. For basic 3D image analysis, we used public domain programs such as SLICE [5] or ImageJ [6]. Image segmentation and cluster labeling were used to extract the microstructure of interest from the digitized image. Segmentation allows us to identify and separate the void space from the solid matrix. For example, global thresholding, the easiest and usual method of segmentation, is done by visiting each pixel (or voxel) in a 8-bit image, and setting the pixel to a grayscale value (e.g., GSV = 255) if its value is above or equal to a given threshold value, and to another grayscale value (e.g., GSV = 0) if the pixel value is below the threshold value.

On the other hand, cluster labeling is an image analysis technique for determining the connectivity of the voxels associated with the microstructure of interest such as the void space or cracks. This cluster labeling analysis allows us to identify the largest percolating cluster, as well as, the other smaller isolated or poorly connected clusters. The algorithm of Hoshen and Kopelman [7] for multiple cluster labeling technique was used along with the 6-point connectivity rule. Using this rule, when a void voxel, for example, is orthogonally in face-to-face contact with another void voxel, the two voxels are considered to be connected whereas if the void voxels are in contact only at the vertex or edge, then the said voxels are considered to be disconnected.

Quantification of Tortuosity

Given that cementitious materials at microscopic scale can be considered as porous media, a typical characteristic of any material transport in this media is the actual path followed by the transported material that is very complicated or so-to-speak tortuous. The concept of tortuosity is generally used in the context of solving the closure problem for transport in porous media, i.e., to derive the macroscopic transport equations in terms of averaged quantities alone [8]. In a capillary model of porous media, tortuosity is introduced as a fudge factor to account for the more complicated transport paths that were neglected in the model.

One of the usual ways of defining tortuosity is that of the ratio of the average length of true transport paths to the length of the system in the direction of the macroscopic flux. In fact, this definition of tortuosity depends not only on the path geometry, but also on the transport mechanism under consideration. In the context of diffusion, tortuosity can be used to describe the longer connecting path imposed by obstacles within the porous media relative to that motion in unconstrained free space. Nevertheless, it is also possible to define tortuosity without any reference to a specific transport mechanism. This could be done, for example, by considering the shortest continuous paths between any two points within the pore space [8].

This study uses the random walk simulation in the digitized void space to quantify diffusion tortuosity. It has been suggested that the time-dependent self-diffusion coefficient $D(t)$, i.e., associated with the random Brownian motion of non-sorbing walkers, can be used to probe the geometry of void space. Diffusion tortuosity is defined as the ratio of the self diffusion coefficient of the walkers in free space (100 % void space) to the long-time self diffusion coefficient of these walkers in void space of the solid matrix. A diffusion tortuosity in free space without any solid obstruction is one whereas in void or pore space in a solid matrix, the value is expected to be greater than one. The higher the diffusion tortuosity is, the higher the resistance to flow or transport within the volume is.

The algorithm for random walk simulation in a 3D lattice proceeds as follows [3,9]: a walker migrates on discrete voxel that corresponds to the void space. A void voxel is chosen randomly as the start position of the lattice walk trial at integer time equals to 0. The walker then executes a random jump to one of the nearest pore voxels and the time of lattice walk is incremented by a unit integer time after the jump. If the randomly selected

voxel is a solid voxel, the jump is not performed but the time is still incremented by one unit. This describes the restricted motion analogous to that of the ‘blind ant trying to escape in the labyrinth’ to simulate the diffusion of a particle in a disordered media as described in percolation theory.

The operational definition of self-diffusion coefficient in a cubic lattice uses the following equation [3,9]:

$$D(t_D) = \frac{1}{6} \frac{d\langle r^2 \rangle}{dt_D}$$

where t_D refers to the dimensionless lattice walk time. Note that the symbol $\langle \rangle$ denotes the average over all the initial and final positions of the walkers and the mean square displacement $\langle r^2 \rangle$ is computed as follows:

$$\langle r(t_D)^2 \rangle = \frac{1}{n} \sum_{i=1}^n \left[(x_i(t_D) - x_i(0))^2 + (y_i(t_D) - y_i(0))^2 + (z_i(t_D) - z_i(0))^2 \right]$$

where n is the number of walkers placed initially at random within the lattice space and x , y , and z are the 3D coordinates of the walker’s position at time t_D for the i th walker.

Application to Deteriorated Cementitious Materials

Frost-induced Damaged Mortar

The material studied was a non-air-entrained fly ash mortar with a fly ash replacement of 30 %, a water-to-binder ratio of 0.50 and a sand-to-binder ratio of 2.50 [2]. The cement used was an ordinary Portland cement (OPC) designated as JIS R5210 whereas the fly ash is of JIS type II. The river sand used in the mixture is of sizes that range from 0.15 mm to 2 mm. In accordance to JIS R5201, the casting in 4 cm x 4 cm x 16 cm steel molds was done. After removing the mortar from the mold, it was cured under water. Then after 14 days of curing, a 12-mm cored sample was obtained from the hardened mortar specimen. A cylindrical specimen with aspect ratio (L/D) of 2 was prepared for the freezing-thawing experiment and X-ray scanning.

In the freezing-thawing experiment, the cylindrical specimen was cyclically exposed to freezing in water at -25°C and then thawing in water at 25°C in an air-temperature controlled room. One cycle of the freezing and thawing took about 12 hours. After a specified number of freeze-thaw cycles, the specimen was removed from the controlled room, and then scanned with microfocus X-ray CT.

The reconstructed CT data obtained from cone beam scanning of the central portion of the cylindrical specimen is shown in Figure 2. In this data set, 199 contiguous slices were obtained such that each slice has a thickness of 40 μm . Stacking up these slices creates the 3D image of the scanned section of the specimen. Each slice or cross-sectional image consists of 1024 x 1024 pixels with a square pixel size of 12 μm .

Figure 3 illustrates the sample cross-sectional images of the mortar specimen after 35 freezing-thawing (FTC) cycles. In this figure, the entrapped air voids and cracks were shown as black whereas the cement pastes were imaged as dark gray. On the other hand, the aggregates (sand) were imaged as patches of different shades of gray in the CT images. Most of the cracks meander around the aggregates suggesting that the internal cracks attempt to follow the weaker interfacial transition zone (ITZ) between the sand and the cement paste in the frost-damaged mortar.

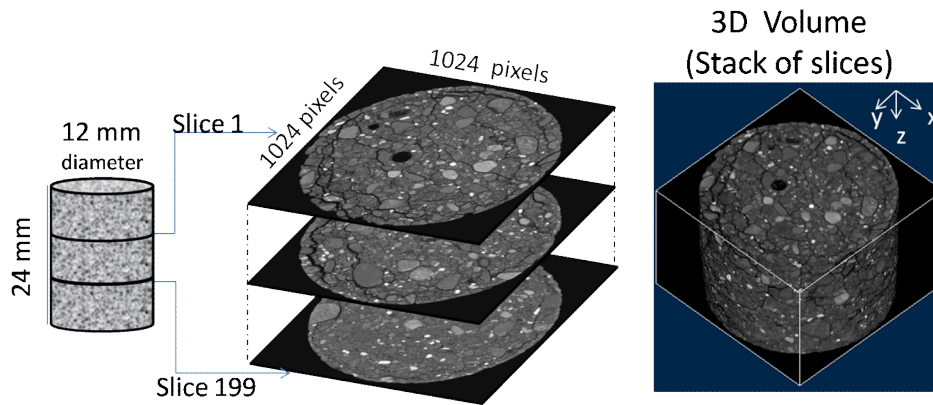


Figure 2. The 3D image obtained from microfocus X-ray CT

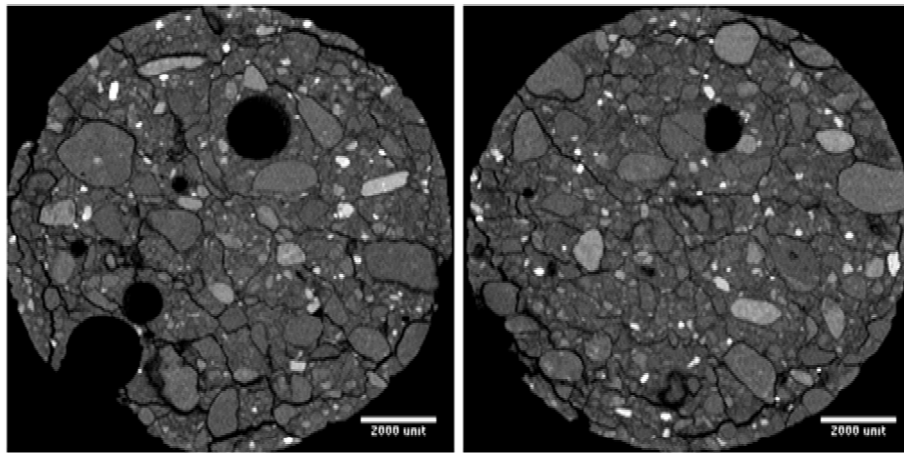


Figure 3. Sample slice of frost-induced damaged mortar after 35 freezing-thawing cycles

Figure 4 illustrates the series of image analysis routines that were applied to the CT images to identify and separate the void space from the solid matrix. The void fraction of the scanned specimen was quantified by dividing the total number of internal void voxels (e.g., black in Figure 4e) with the total number of foreground voxels (e.g. black in Figure 4d). In addition, connectivity analysis through multiple cluster labeling of the void voxels were done to evaluate the degree of connectivity of the void space. This connectivity parameter was estimated from the ratio of the volume of largest void cluster to that of the total void space. The degree of connectivity would therefore be 1.0 if all the void voxels (i.e. air voids and cracks) are connected to each other to form only one large void cluster.

Figure 5 illustrates the void space of the undamaged mortar and the damaged mortar in three dimensions. At the early stage of FTC, no clear cracks were observed and the measured void space was found to be 1.3 % of the volume of the scanned specimen. This value seems to be reasonable for the initial air content of non-air-entrained mortars and a significant increase of void space (6.3%) was then measured at 35 FTC because of the formation of internal cracks as seen from the CT images. Moreover, the degree of void connectivity increased from 0.3 to 0.8 at 35 FTC, indicating that about 80 % of the void space (individual air voids and cracks) forms a well-connected crack system in three dimensions. Note that the voxels rendered in white (see Figure 5 and 6c) is identified as the largest cluster within the VOI.

To further characterize the connected crack system, a volume of interest (VOI) was extracted as shown in Figure 6. Random walk in the void space was simulated to quantify diffusion tortuosity in the connected crack system. Based from the results of 3D random walk simulation in the cubic lattice space of the VOI, the diffusion tortuosity in x, y and z directions are estimated to be 6.2, 7.1 and 15.8, respectively; suggesting crack anisotropy in 3D [10].

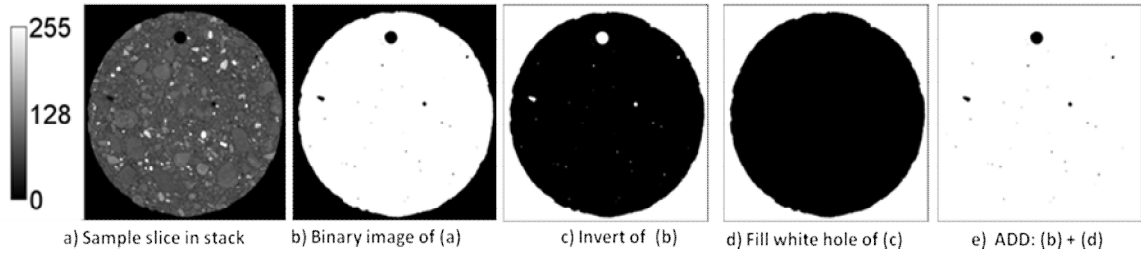


Figure 4. Extraction of void voxels from the solid matrix

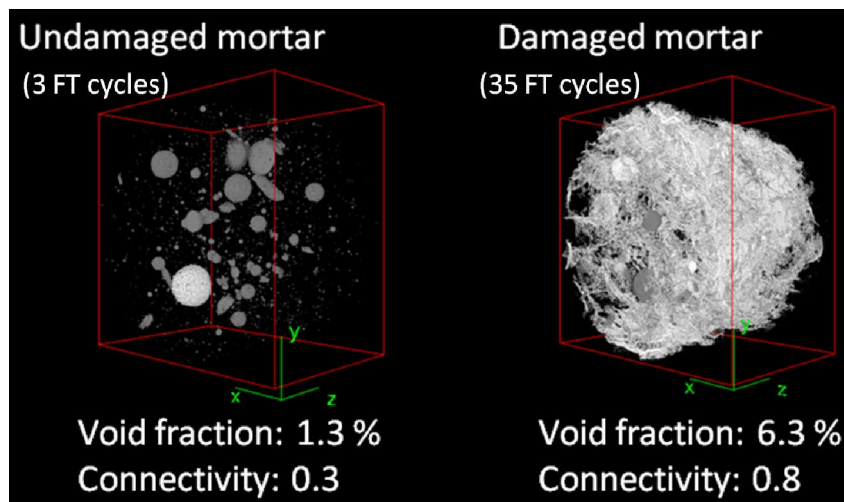


Figure 5. Visualization and quantification of void space in 3D

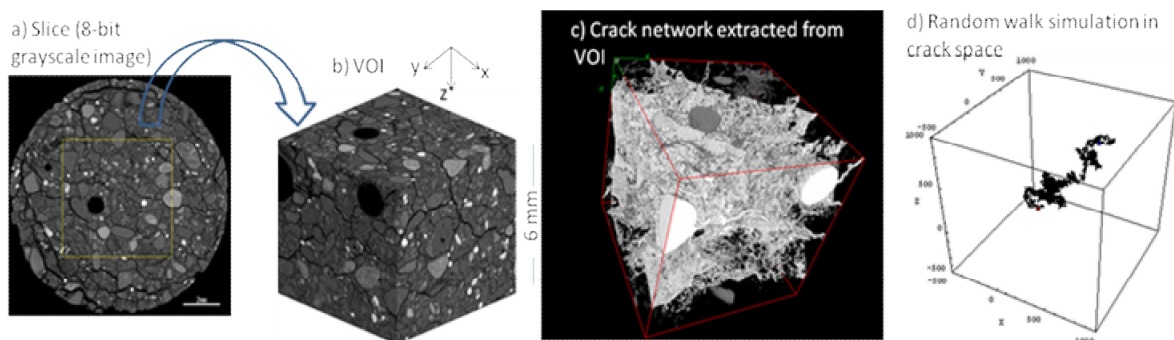


Figure 6. Analysis of crack network from the volume of interest (VOI)

Deteriorated Mortar Due to Calcium Leaching

The material studied was an ordinary Portland cement mortar with a water-to-cement ratio of 0.50, and a sand (maximum particle size of 210 μm) to cement ratio of 2.0. The test specimen was cured further for about 24 weeks before it was subjected to an accelerated leaching test. This leaching test based on the principle of electrochemical migration is shown to simulate the long-time degradation of cementitious material due to leaching of calcium ions when in contact with water [11-12]. The application of electrical field accelerates the dissolution of hydrated cement products such as portlandite as the cations such as the Ca^{2+} move rapidly to the cathode side. After the accelerated leaching test of the sample for 13 weeks, the deteriorated cement paste nearest to the cathode side was also cut in preparation for CT scanning. A shard of about 1 mm at its greatest width and 1 mm in length were prepared as test specimen for synchrotron microtomography. After scanning the specimen, the 3D image of its internal structure was obtained. The reconstructed 3D-image data set was composed of 1300 contiguous grayscale images where each slice image contained 2000 x 2000 voxels. The effective size of a cubic voxel in the CT image is 0.50 μm .

Figure 7 shows the sample slice and a representative volume of interest (VOI) from where the largest percolating pore cluster was extracted. Results indicate that about 98 % of the identified pore voxels (labeled as blue) in the VOI of DM are connected to each other and to the surface or faces of VOI whereas the other 2 % (labeled as green) are smaller isolated or dead-end pore clusters. The effective porosity associated with this largest percolating pore cluster is computed to be 0.38. This increased porosity may be due to the dissolution of hydrated cement products such as portlandite (calcium hydroxide) as calcium leached out from the cement matrix. Such connected pore space would most likely contribute to the macroscopic transport in the deteriorated mortar.

Output from the random walk simulation in the VOI using 50,000 walkers at a maximum lattice walk time of 2 million is also shown in Figure 8. In Figure 8b, the slope in these plots at long lattice-walk time provides an estimate of the normalized self-diffusion coefficient (relative to free space), which is the reciprocal of diffusion tortuosity. Accordingly, the diffusion tortuosity in free space (i.e. 100% porosity) and the percolating pore space (38 % porosity in VOI) was computed to be about 1.0 and 3.7, respectively [11].

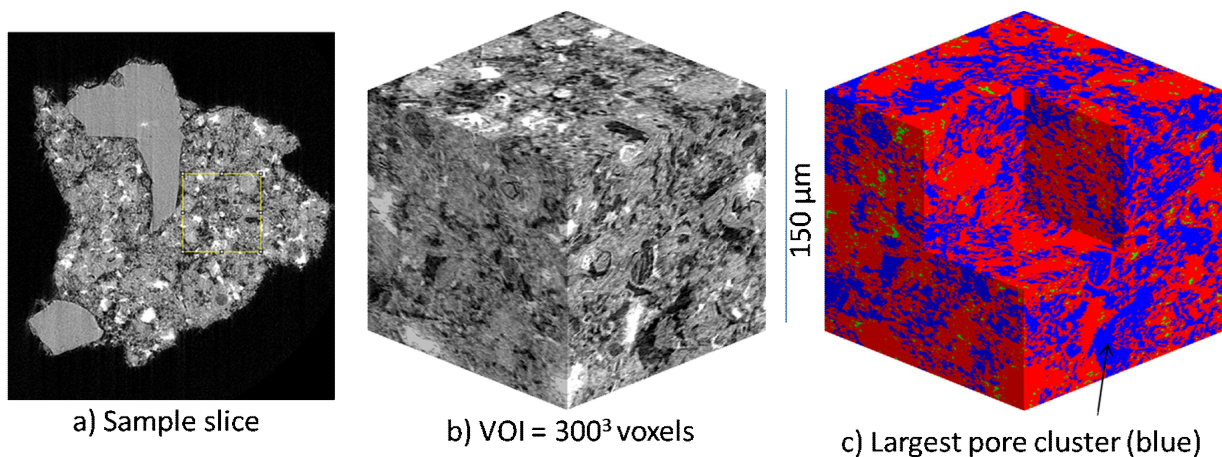


Figure 7. Analysis of CT image obtained from synchrotron microtomography

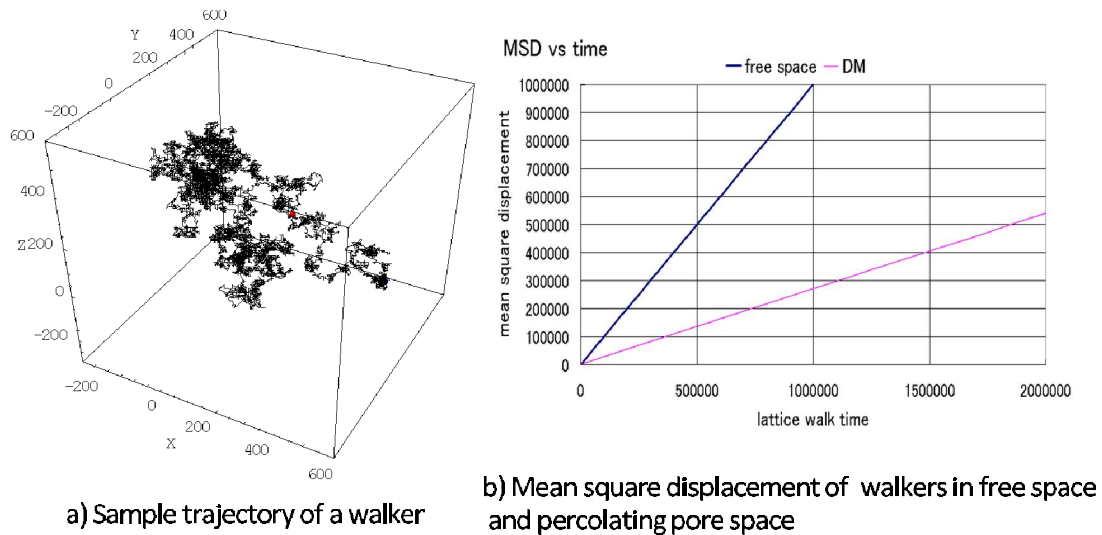


Figure 8. Output from random walk simulation in 3D pore space

Conclusions

Visualization and quantification of the microstructure of cementitious materials in three dimensions without physically cutting the specimen into thin sections were made possible using X-ray microtomography. It allows us to characterize the cracks that could be formed from frost-induced damaged mortar at a spatial resolution of 12 μm using microfocus X-ray CT. It also allows us to characterize the pore structure in deteriorated mortar due to calcium leaching at a spatial resolution of 0.5 micron using synchrotron microtomography. Moreover, the information obtained from the analysis of digitized images allows us to measure 3D parameters such as the connectivity and tortuosity of void, crack or pore space. Indications suggest that the cracks from frost-induced damaged mortar form a well-connected network of void space. Likewise, a well-connected pore network that forms most likely from the dissolution of hydrated cement products was also observed from a deteriorated mortar where calcium ions are leaching out. Such microstructure characteristics would play a significant role in the macroscopic properties of these materials particularly its transport properties like diffusivity and permeability. Thus, such studies would hopefully serve as an impetus for utilization of this technique to understand further the relationship between the microstructure and the durability performance of cementitious materials.

Acknowledgments

Part of this research is funded from the author's postdoctoral fellowship of the Japan Society for the Promotion of Science (JSPS). The author also acknowledges Professor Sugiyama who serves as my host researcher during the course of these studies.

References

- [1] M.A.B. Promentilla, and T. Sugiyama, "Microstructure characterization of cement-based materials using X-ray microtomography," In: *The 3rd Regional Conference on Chemical Engineering*, Mandaluyong City, Manila, Philippines, 2011.
- [2] M.A.B. Promentilla, and T. Sugiyama, "X-ray microtomography of mortars exposed to freezing-thawing action," *Journal of Advanced Concrete Technology*, Japan Concrete Institute, Vol. 8, No. 2, pp. 97-111, 2010.

- [3] M.A.B. Promentilla, T. Sugiyama, T. Hitomi, and N. Takeda, "Quantification of tortuosity in hardened cement pastes using synchrotron-based X-ray computed microtomography," *Journal of Cement and Concrete Research*, Vol. 39, pp. 548-557, 2009.
- [4] K. Uesugi, Y. Suzuki, N. Yagi, A. Tsuchiyama, and T. Nakano, "Development of high spatial resolution X-ray CT system at BL47XU in SPring-8," *Nuclear Instruments and Methods I Physics Research A*, Vol. 467-468, No. 2, pp. 853-856, 2001.
- [5] T. Nakano, A. Tsuchiyama, K. Uesugi, M. Uesugi, and K. Shinohara, "SLICE software for basic 3-D image analysis," Japan Synchrotron Radiation Research Institute (JASRI), 2006. [Online]. Available: <http://www-bl20.spring8.or.jp/slice/>, [Accessed: May 2007].
- [6] W. Rasband "ImageJ: Image processing and analysis in Java," National Health Institute, 2007. Available: <http://rsb.info.nih.gov/ij/>, [Accessed: May 2007].
- [7] J. Hoshen, and R. Kopelman, "Percolation and cluster distribution. I. Cluster multiple labeling technique and critical concentration algorithm," *Physical Review B*, Vol. 14, pp. 34-38, 1976.
- [8] A. Koponen, M. Kataja, and J. Timonen, "Tortuous flow in porous media," *Physical Review E*, Vol. 54, No. 1, pp. 406-410, 1996.
- [9] Y. Nakashima, and S. Kamiya, "Mathematica programs for the analysis of three-dimensional pore connectivity and anisotropic tortuosity of porous rocks using X-ray microtomography," *Journal of Nuclear Science and Technology*, Vol. 44, No. 9, pp. 1233-1247, 2007.
- [10] M.A.B. Promentilla, and T. Sugiyama "Computation of crack tortuosity from microtomographic images of cement-based materials," In: *The 12th International Conference on the Enhancement and Promotion of Computational Methods in Engineering and Science (EPMESC XII)*, Hong Kong and Macau, 2009.
- [11] M.A.B. Promentilla, T. Sugiyama, T. Hitomi, and N. Takeda, "Pore space analysis and estimation of transport properties of deteriorated cementitious material using synchrotron microtomography," In: *The 2nd International RILEM Workshop on Concrete Durability and Service Life Planning (ConcreteLife 2009)*, Haifa, Israel, pp. 498-506, 2009.
- [12] T. Sugiyama, M.A.B. Promentilla, T. Hitomi, and N. Takeda, "Application of synchrotron microtomography for pore structure characterization of deteriorated cementitious materials due to leaching," *Cement and Concrete Research*, Vol. 40, No. 8, pp. 1265-1270, 2010.